npj | systems biology and applications

Article

Published in partnership with the Systems Biology Institute

https://doi.org/10.1038/s41540-024-00443-4

Experimentally-driven mathematical model to understand the effects of matrix deprivation in breast cancer metastasis

Sayoni Maiti[1], Annapoorni Rangarajan[2] ✉ & Venkatesh Kareenhalli[3] ✉

Normal epithelial cells receive proper signals for growth and survival from attachment to the underlying extracellular matrix (ECM). They perceive detachment from the ECM as a stress and die — a phenomenon termed as 'anoikis'. However, metastatic cancer cells acquire anoikis-resistance and circulate through the blood and lymphatics to seed metastasis. Under normal (adherent) growth conditions, the serine-threonine protein kinase Akt stimulates protein synthesis and cell growth, maintaining an anabolic state in the cancer cell. In contrast, previously we showed that the stress due to matrix deprivation is sensed by yet another serine-threonine kinase, AMP-activated protein kinase (AMPK), that inhibits anabolic pathways while promoting catabolic processes. We illustrated a switch from $Akt^{high}/AMPK^{low}$ in adherent condition to $AMPK^{high}/Akt^{low}$ in matrix-detached condition, with consequent metabolic switching from an anabolic to a catabolic state, which aids cancer cell stress-survival. In this study, we utilized these experimental data and developed a deterministic ordinary differential equation (ODE)-based mechanistic mathematical model to mimic attachment-detachment signaling network. To do so, we used the framework of insulin-glucagon signaling with consequent metabolic shifts to capture the pathophysiology of matrix-deprived state in breast cancer cells. Using the developed metastatic breast cancer signaling (MBCS) model, we identified perturbation of several signaling proteins such as IRS, PI3K, PKC, GLUT1, IP3, DAG, PKA, cAMP, and PDE3 upon matrix deprivation. Further, in silico molecular perturbations revealed that several feedback/crosstalks like DAG to PKC, PKC to IRS, S6K1 to IRS, cAMP to PKA, and AMPK to Akt are essential for the metabolic switching in matrix-deprived cancer cells. AMPK knockdown simulations identified a crucial role for AMPK in maintaining these adaptive changes. Thus, this mathematical framework provides insights on attachment-detachment signaling with metabolic adaptations that promote cancer metastasis.

Cancer can be perceived as a state of human cells whereby they have transitioned from normalcy to neoplastic growth and malignancy aided by the accumulation of genetic and epigenetic changes[1]. GLOBOCAN 2020 cancer statistics reveal that female breast cancer contributes to the majority (11.7%) of all cancer incidences when compared across both sexes[2]. Among females, breast cancer not only makes up for the majority of incidences, but also contributes to the majority of cancer-associated deaths worldwide[2]. It is estimated that around 90% of cancer-associated mortalities are due to metastasis[3] – the process by which cancer cells detach from the primary site, intravasate into the vasculature, survive in the circulation, extravasate at a secondary site and develop into a secondary tumor (illustration in Fig. 1). Understanding the underlying molecular mechanisms of this multi-step invasion-metastasis cascade can help curb the spread of cancer, and thus, cancer-associated mortality.

Epithelial cells are attached to the underlying extracellular matrix (ECM) through cell surface proteins called integrins[4]. This attachment is necessary for receiving adequate signals for growth and survival. When cells are adhered to the ECM, under normal growth conditions, the PI3K/Akt/mTOR signaling pathway promotes nutrient uptake, protein synthesis, and cell proliferation, thus maintaining an anabolic state in the cancer cell[5].

[1]Interdisciplinary Programme in Mathematical Sciences, IISc Mathematics Initiative, Indian Institute of Science, Bengaluru, India. [2]Department of Developmental Biology and Genetics, Indian Institute of Science, Bengaluru, India. [3]Department of Chemical Engineering, Indian Institute of Technology Bombay, Mumbai, India. ✉e-mail: anu@iisc.ac.in; venks@iitb.ac.in

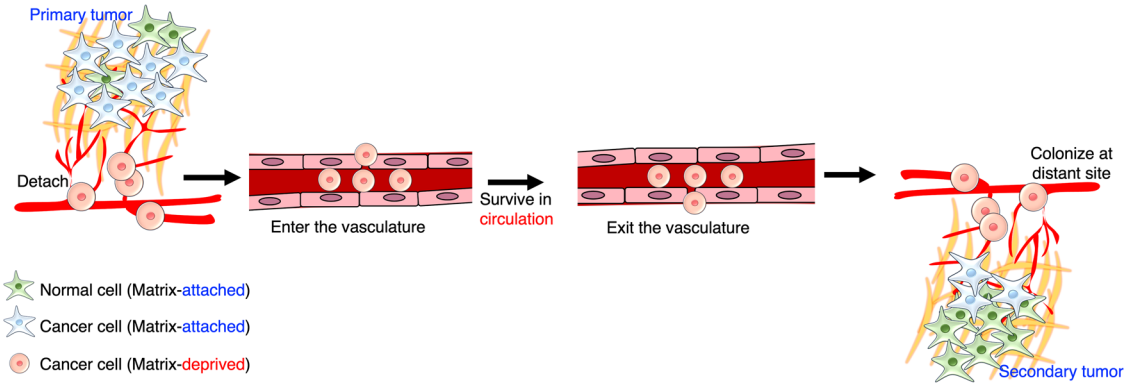

Fig. 1 | Process of metastasis. Metastasis is defined as the process by which cancer cell detach from the primary site, enter into the vasculature, survive in circulation, exit from the vasculature and colonize at a secondary site.

The cells perceive detachment from the underlying ECM as a stress, which leads to cell death. This cell death due to matrix deprivation is known as anoikis[6]. In contrast to normal cells, cancer cells acquire the ability to overcome anoikis, which enables their exit from the primary site and journey through the circulation to seed metastasis. Following the disruption of cell-ECM interaction, cancer cells encounter multiple stresses including altered mechanical forces, cytoskeletal rearrangement, and shear stress[7]. We recently showed that one protein that senses matrix detachment stress is the metabolic regulator AMP-activated protein kinase (AMPK)[8–10]. AMPK is activated by two main upstream kinases - Liver Kinase B1 (LKB1) which appears to be constitutively active[11], and Calcium/Calmodulin-dependent protein kinase kinase beta (CaMKKβ) which is activated by increase in intracellular calcium concentration[11]. Upon activation, AMPK promotes catabolic pathways like fatty acid oxidation and glycolysis, while simultaneously inhibiting anabolic pathways such as protein synthesis, fatty acid synthesis and glycogen synthesis[12]. Thus, survival under matrix deprivation involves an interplay among alterations in mechanotransduction, biophysical forces, signaling molecules, and metabolic alterations. To better understand the complexity of the underlying signal transduction networks that govern the adaptation of cancer cells to matrix deprivation, in this study, we have taken a mathematical modeling approach which serves as a powerful tool to investigate molecular responses systematically.

One of the earliest mathematical models of tumor invasion and metastasis described tumor in macro-scale structure (cell population level) and micro-scale structure (individual cell level) and used partial differential equations describing the synthesis and/or activation of matrix-degrading enzymes by the tumour cells to model invasion, migration and angiogenesis[13]. A recent report on modeling metastasis captured the interconnected process of invasion and metastatic spread of individual cancer cells in a spatially explicit manner[14]. Mathematical models on breast cancer tumor progression with respect to immune infiltration[15] and cell cycle events[16] have also been attempted. Experimentally-driven mathematical models have elucidated targeted therapy for HER2+ breast cancer[17], Warburg phenotype in breast cancer[18], and metabolic plasticity by coupling gene regulation with metabolic pathways[19]. Few of these models have explained intracellular signaling network and elucidated treatment responses of cancer cells to several drugs using model simulations. However, all the above studies were restricted to matrix-attached or adherent cell culture systems. One recent work from our laboratory integrated computational-experimental approach and developed a mechanism-based mathematical model that captures the set of experimentally reported interactions among the kinases AMPK/Akt, and their respective phosphatases PP2C/PHLPP2, and showed the existence of bistability over a specific range of parameter sets[20]. To the best of our knowledge, there exists no mathematical model that captures the attachment-detachment signaling network and attributes to the metabolic states of matrix-attached and matrix-deprived breast cancer cells.

Development of metastatic breast cancer signaling (MBCS) mathematical model to simulate matrix deprivation in breast cancer cells

In this study, we developed an experimentally-driven, deterministic, ODE-based, mechanistic mathematical model that captures the pathophysiology of matrix-deprived breast cancer cells, and is referred to as the metastatic breast cancer signaling (MBCS) model. To do so, we combined the experimental data on attachment-detachment signaling comprising of AMPK-Akt crosstalk in matrix-deprived breast cancer cells[10], and concepts of a computational model on integrated insulin-glucagon signaling network[21], as described below.

Prior experimental work from our laboratory identified that detachment of adherent breast cancer cells by trypsinization or mechanical scraping leads to AMPK activation (Fig. 2a). We further demonstrated that the spike in cytosolic calcium (Ccal) levels induced by matrix detachment contributes towards the rapid and sustained activation of AMPK via CaMKKβ[9]. We additionally showed that matrix deprivation-triggered AMPK activity concomitantly inhibits Akt activity. The resultant $AMPK^{High}/Akt^{Low}$ state was essential for the stress-survival of matrix-detached breast cancer cells[10]. Coupling the AMPK/Akt activity states with transcriptomics data analyses, we also reported that matrix-attached and matrix-deprived conditions were associated with anabolic and catabolic states, respectively[10]. Furthermore, we recently showed the inhibition of mTOR (a key player in protein synthesis) and consequent impairment of protein synthesis upon matrix deprivation[22]. These experimental data are depicted as a cartoon in Fig. 2a.

To create a mathematical model that captures the above effects of matrix deprivation, we adapted a mathematical framework on integrated insulin-glucagon signaling pathway[21] as illustrated in Fig. 2b. Somvanshi et al. explained the signaling of IRS/PI3K/PKC and IRS/PI3K/Akt/mTOR pathways activated by insulin, and cAMP/PKA and PLC pathways activated by glucagon[21]. They further described the outcome of these signaling pathways as anabolic and catabolic state based on the activation state of Akt and PKA, respectively. Insulin signaling via the PI3K-Akt signaling pathway increases glucose uptake via GLUT4, promotes glycogenesis and stimulates fat synthesis, thus contributing to the anabolic state of the cell[23,24]. On the contrary, glucagon signaling, via the activation of PKA, promotes glycogenolysis and gluconeogenesis while inhibiting glycogenesis and glycolysis[25], thereby contributing to a catabolic state within the cell[24,25]. A Hill function in terms of pAkt (phosphorylated Akt) was used to quantify the anabolic state and a Hill function in terms of aPKA (active PKA) was used to quantify the catabolic state[21]. The saturation constants of these functions were calibrated and fixed at the physiological range as reported previously[21]. The signaling network was triggered by the levels of macronutrients like glucose, amino acid and fatty acid in coordination with hormones like insulin and glucagon[21].

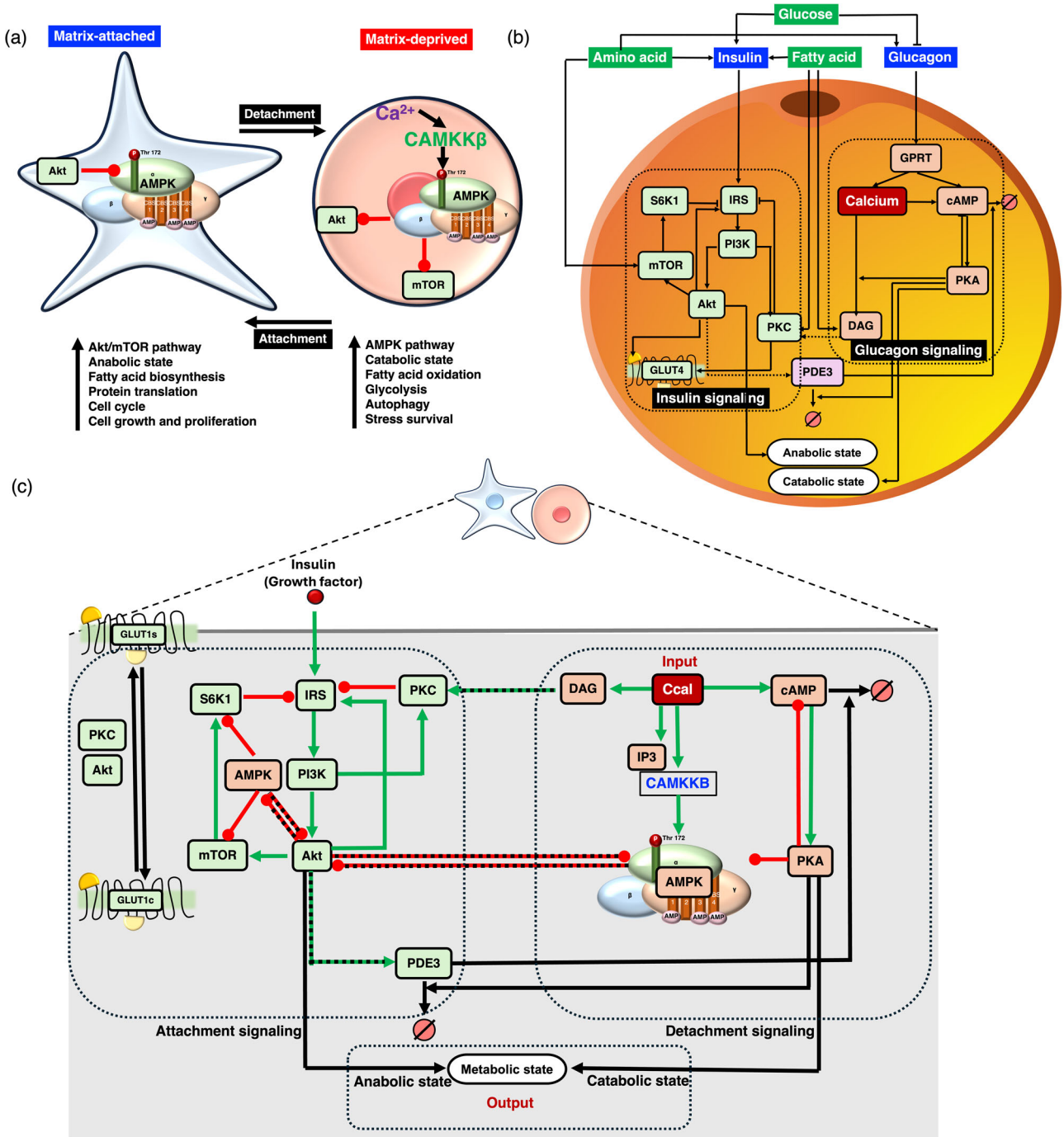

Fig. 2 | Development of metastatic breast cancer signaling (MBCS) mathematical model to simulate matrix deprivation in breast cancer cells. a Cartoon depicting AMPK-Akt signaling in matrix-attached vs matrix-detached breast cancer cells: (adapted and modified from Saha et al., 2018: In matrix-attached condition, active Akt inhibits AMPK and maintains $pAkt^{High}/pAMPK^{Low}$ phenotype which corresponds to anabolic state and is conducive for cell growth and proliferation. In matrix-deprived condition, the spike in cytosolic calcium (Ccal) triggered by matrix-detachment activates AMPK via CAMKKβ. Active pAMPK inhibits Akt and maintains $pAMPK^{High}/pAkt^{Low}$ phenotype which corresponds to catabolic state that facilitates stress-survival in matrix-deprived cancer cells. **b** Cartoon depicting integrated insulin-glucagon signaling network (adapted and modified from Somvanshi et al., 2019). The inputs to the cell consisted of glucose, amino acid and fatty acids as macronutrients present in the plasma whose levels trigger hormones like insulin and glucagon, and their signaling, respectively. When insulin signaling is switched on, the metabolic state is anabolic. When glucagon signaling is switched on, the metabolic state is catabolic. **c** Proposed network on attachment-detachment signaling in breast cancer cells. In the matrix-attached state, growth factors like insulin activate the IRS/PI3K/Akt axis and consequent increase in pAkt levels maintains an anabolic state in the cell. The signaling molecules that are functional in the matrix-attached state constitute the attachment signaling and include IRS, PI3K, Akt, mTOR, S6K1, PKC, GLUT1 and PDE3. Upon matrix deprivation, the spike in cytosolic calcium activates the cAMP/PKA axis and consequent increase in levels of aPKA maintains a catabolic state in the cell. The signaling molecules that are functional in the matrix-detached state constitute the detachment signaling and include Ccal, CAMKKβ, DAG, IP3, cAMP, PKA and AMPK. Green arrows indicate positive feedback or activation. Red lines ending with a dot indicate negative feedback or inhibition. Black solid lines indicate translocation, degradation, and metabolic states. Black dotted lines indicate crosstalks between anabolic and catabolic pathways.

We drew parallels between the AMPK-Akt crosstalks and metabolic states of breast cancer cells (Fig. 2a) with the signaling molecules and metabolic states regulated by the insulin-glucagon pathway (Fig. 2b) and propose an integrated attachment-detachment signaling network (Fig. 2c) for the MBCS model.

The following key modifications were made to the existing insulin-glucagon mathematical framework[21] to capture the effects of matrix deprivation on breast cancer cells. Firstly, the equation of Akt was modified to include the negative effect of AMPK on Akt. CaMKKβ was introduced as an upstream kinase of AMPK. The effect of the spike in cytosolic calcium was transferred to AMPK via CaMKKβ. GLUT4 was replaced by GLUT1 since it is the glucose transporter predominantly expressed in breast cancer cells. AMPK's negative effect on mTOR was captured by modifying the equation of mTOR. Selected parameters were adjusted to get the relative fold changes of pAMPK, pAkt and p-mTOR in matrix-deprived compared to matrix-attached condition (see Methods). This model describes breast cancer cells in matrix-attached vs. matrix-deprived condition as follows: in the matrix-attached state, growth factors like insulin activate the IRS/PI3K/Akt axis and consequent increase in pAkt levels maintains an anabolic state in the cell. The signaling molecules that are functional in the matrix-attached state constitute the attachment signaling and include IRS, PI3K, Akt, mTOR, S6K1, PKC, GLUT1 and PDE3. Upon matrix deprivation, the spike in cytosolic calcium activates the cAMP/PKA axis and consequent increase in levels of aPKA maintains a catabolic state in the cell. The signaling molecules that are functional in the matrix-detached state constitute the detachment signaling and include Ccal, CAMKKβ, DAG, IP3, cAMP, PKA and AMPK. Interactions within a signaling pathway are referred to as feedbacks, such as, IRS to PI3K, PI3K to Akt, Akt to IRS, PI3K to PKC, PKC to IRS, S6K1 to IRS, Akt to mTOR, mTOR to S6K1, Ccal to DAG, Ccal to cAMP, Ccal to IP3, Ccal to CAMKKβ, cAMP to PKA, and PKA to AMPK. When activation of one pathway produces an effect on another pathway, this phenomenon is known as crosstalk[26]. In Fig. 2c, there are three crucial crosstalks between the attachment signaling/anabolic pathway and detachment signaling/catabolic pathway namely: DAG to PKC, Akt to PDE3 and AMPK to Akt. Further, since AMPK and Akt reciprocally and negatively regulate each other, the interaction between AMPK and Akt also constitutes a double-negative feedback loop[10].

Since matrix detachment leads to a spike in cytosolic calcium (Ccal) thereby activating AMPK, we denoted the spike in Ccal as a surrogate for matrix deprivation. Thus, in our model we used alteration in Ccal level as the input, and metabolic state (anabolic and catabolic states) as the output. We calibrated the MBCS model using experimental data on pAMPK, pAkt, p-mTOR upon matrix detachment. Influential parameters were estimated by fitting the model to these experimental data. We validated the model using data from independent experiments on protein levels, metabolic states, and AMPK down-modulation (as discussed in the Results section). All experimental data used in the model calibration and validation were in vitro experiments done using metastatic breast cancer MDA-MB-231 cell line that were subjected to matrix detachment for 8 to 24 h. All the data used for model calibration and model validation are summarized in Supplementary Information section as Supplementary Table 1. Details on the mathematical model building is given in the Methods section. Details on equations capturing molecular interactions, kinetic parameters and initial concentrations, as documented in the literature[21] are provided in the Supplementary Information section. We propose that this model captures the attachment-detachment signaling network of breast cancer cells and is sufficient to explain important experimental observations on the molecular interplay and metabolic states in matrix-deprived condition.

Results

The calibrated and validated mathematical model captures the intracellular signaling network of matrix-deprived breast cancer cell

For model calibration, we identified intracellular signaling molecules which were perturbed upon matrix deprivation. Details on experimental data extraction are mentioned in the Methods section. Using MDA MB 231 invasive breast cancer cells, previous work from our laboratory showed that matrix deprivation triggers a spike in cytosolic calcium which causes a rapid and sustained activation of AMPK by its upstream kinase CaMKKβ[9], which in turn decreases the activity of Akt[10] and mTOR[22] (Fig. 2a). Therefore, matrix detachment-triggered spike in intracellular calcium was used as input to initiate the development of MBCS mathematical model. The model was simulated for 10 min in adherent state following which detachment was initiated (indicated by black arrow in Fig. 3), and the model behaviour was compared with the experimental data. The model (solid black lines in Fig. 3) quantitatively captured the foldchange of cytosolic calcium upon detachment (Fig. 3a), and that of phosphorylated and thus active forms of AMPK (pAMPK; Fig. 3b), Akt (p-Akt; Fig. 3c), and mTOR (p-mTOR; Fig. 3d), demonstrating a good agreement with the experimental results (red stars in Fig. 3). Thus, the developed MBCS mathematical model faithfully recapitulated the dynamics of matrix detachment-induced calcium spike leading to AMPK activation and consequent inactivation of Akt and mTOR.

We further validated the MBCS model by asking if the outcomes of the model conform to other known experimental observations. Prior work from the lab, and other data from the literature, showed that matrix-detachment results in decreased phosphorylation of S6K1[22], no change in PKC activity (Supplementary Fig. 1) while increase in the activity of PKA[27]. Indeed the model outcomes on the temporal dynamics and fold changes of pS6K1 (phospho-S6K1; Fig. 3e), pPKC (phospho-PKC; Fig. 3f), and aPKA (active-PKA; Fig. 3g) were in line with the experimental data.

Additionally, prior transcriptomics-based experimental data from our laboratory showed that genes involved in anabolic processes like fatty acid synthesis, pentose phosphate pathway, mTOR pathway, protein synthesis, cell growth and proliferation were enriched in matrix-attached cells. Conversely, genes involved in catabolic processes including fatty acid oxidation, glycolysis, autophagy, oxidative stress and hypoxia were elevated in matrix-deprived cells[10]. These data showed the existence of metabolic switching from anabolic to catabolic state when breast cancer cells were shifted from matrix-attached condition to matrix-detached condition[10] (Fig. 2a). We queried if similar metabolic shifts are mimicked by the MBCS model. In the attachment-detachment signaling network developed in our study (Fig. 2c), the metabolic state comprises of anabolic and catabolic states attributed to the phosphorylation status of Akt (pAkt) and the activation of PKA (aPKA), respectively. The graph in Fig. 3h shows that the outcome of the model also captures the switch in metabolic state from anabolic to catabolic upon matrix deprivation; the metabolic switch is indicated by the cross-over of blue (anabolic state) and red (catabolic state) lines. Taken together, these data show that the developed mathematical framework is able to capture the molecular dynamics of attachment-detachment signaling and accompanying metabolic alterations.

Model predicts the effects of matrix deprivation on several intracellular signaling molecules of the network

We next implemented the model to explore the effects of matrix deprivation on several intracellular signaling molecules depicted in the attachment-detachment network (Fig. 2c). The model predicted a decrease in the levels of pIRS (phospho IRS; Fig. 4a), aPI3K (active PI3K; Fig. 4b), sGLUT1 (surface GLUT1; Fig. 4c) and aPDE3 (active PDE3; Fig. 4g) upon matrix deprivation. Additionally, the model predicted an increase in IP3 (Fig. 4d), DAG (Fig. 4e), and cAMP (Fig. 4f).

To get a system-level understanding of the attachment-detachment signaling network (Fig. 2c), the MBCS model was used to quantify the strengths of the various interactions capturing the molecular interplay. The resultant network diagram, with the quantification of relative operational strengths of the feedbacks and crosstalks among signaling molecules pathways, is referred to as the flux map (Fig. 5). The operational strengths of the feedbacks and crosstalks (written as numbers along the arrows) were calculated as the absolute values of the corresponding Hill functions, as shown previously[21], that depict the magnitude of the activation and inhibition. The numbers in blue pertain to the matrix-attached condition while

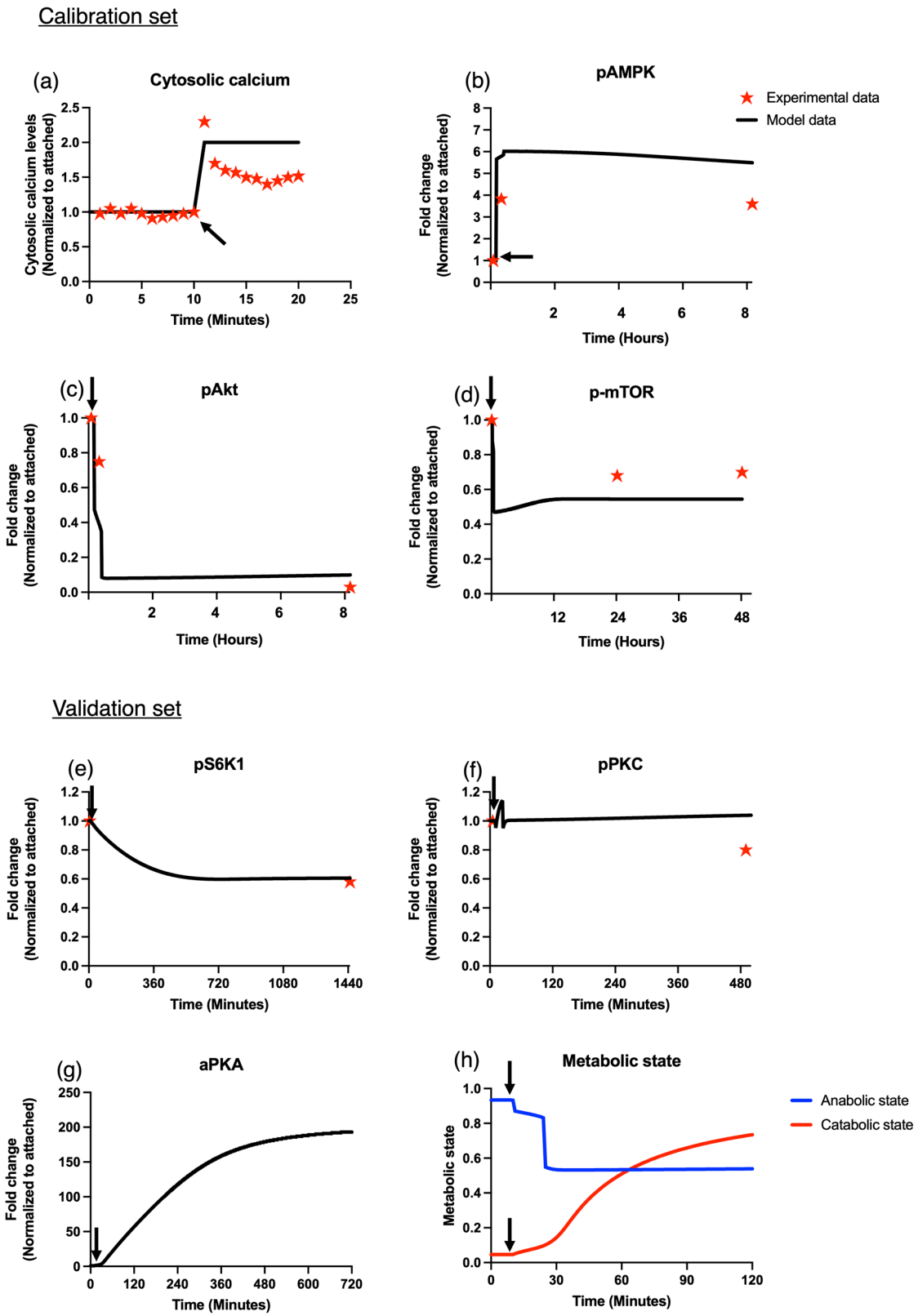

Fig. 3 | Effect of matrix deprivation on temporal dynamics of intracellular signaling molecules. The model calibration set consists of (**a**) spike in cytosolic calcium triggered on matrix deprivation, consequent activation of (**b**) AMPK, and inactivation of (**c**) Akt and (**d**) mTOR. Experimental data is depicted by red stars in the calibration set. The validation set consists of (**e**) pS6K1, (**f**) pPKC, (**g**) aPKA, and (**h**) metabolic state. Model data is shown by black line. The black arrow indicates the time point when matrix deprivation is induced by the spike in cytosolic calcium. The x-axis depicts time in minutes or hours (the range of x-axis is variable, it is based on the time required to attain steady state), where the first 10 min is the matrix-attached state and remaining is the matrix-deprived state. The y-axis in all graphs except (**h**) depicts the fold change of protein levels, normalized to protein levels in the matrix-attached condition.

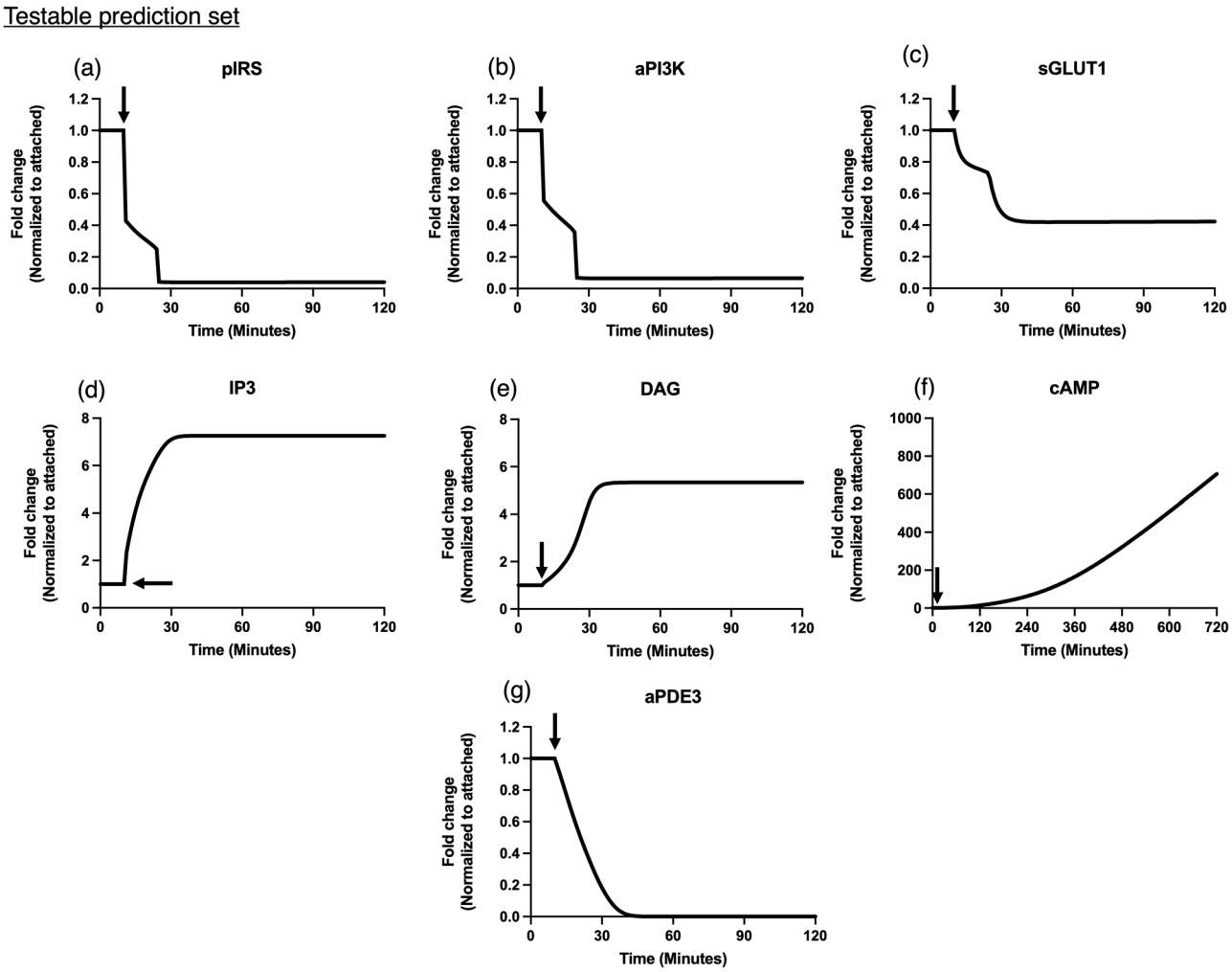

Fig. 4 | Effect of matrix deprivation on temporal dynamics of intracellular signaling molecules. The testable prediction set consists of (**a**) pIRS, (**b**) aPI3K, (**c**) sGLUT1, (**d**) IP3, (**e**) DAG, (**f**) cAMP and (**g**) aPDE3. Model data is shown by black line. The black arrow indicates the time point when matrix deprivation is induced by the spike in cytosolic calcium. The x-axis depicts time in minutes (the range of x-axis is variable, it is based on the time required to attain steady state), where the first 10 min is the matrix-attached state and remaining is the matrix-deprived state. The y-axis depicts the fold change of signaling molecules normalized to matrix-attached condition.

the numbers in red pertain to the matrix-detached state. As the feedbacks and crosstalks are written in terms of Hill functions, the numbers vary between the range of 0 and 1. A value closer to 0 represents mild/low strength of activation or inhibition, while a value closer to 1 represents a strong/high strength of activation or inhibition. A value closer to 0.5 depicts neutral effect.

In adherent cells, binding of growth factor like insulin to its cognate receptor leads to the recruitment and phosphorylation of insulin receptor substrate (IRS). IRS recruits and activates PI3K which further activates Akt and PKC. Upon activation, the PI3K/Akt axis regulates several arms of the signaling network as shown in Fig. 5 (numbers in blue), such as: (1) Upon activation, pAkt activates mTOR/S6K1 arm as well as auto-activates the IRS/PI3K axis, while S6K1 inhibits IRS. (2) Akt and PKC promote the translocation of GLUT1 from the cytosol to the cell surface. (3) pAkt also inhibits AMPK; the remaining low levels of pAMPK shows reduced inhibition on mTOR and S6K1. (4) pAkt also activates PDE3 which promotes the degradation of cAMP; low levels of cAMP fail to activate PKA.

Furthermore, the status of the crosstalks in the matrix-attached state reveals an interesting trend. The crosstalk from catabolic to anabolic pathway (i.e., DAG to PKC) is completely switched off, which indicates low levels of PKC and hence low inhibition of IRS. This manifests into high levels of pAkt. Conversely, the crosstalk from anabolic to catabolic pathway (i.e., Akt to PDE3) is fully operational, which indicates high levels of PDE3 and hence high degradation of cAMP. This manifests into low levels of aPKA. Additionally, the crosstalk from Akt to AMPK is fully functional while the crosstalk from AMPK to Akt is non-functional. Therefore, in the matrix-attached state, the anabolic signaling is fully functional with high Akt activation, higher GLUT1 on the membrane for glucose transport, while low AMPK levels and low PKA indicate catabolic signaling is switched off. Taken together, the flux map (Fig. 5; numbers in blue values) captures the signaling status of matrix-attached cells.

Matrix-detachment triggers calcium spike and promotes AMPK activation via CaMKKβ[9]. Classical GPCR signaling activates PLC which then is broken down into IP3 which also results in intracellular release of Calcium from the ER store[28]. The MBCS model predicts that the elevated levels Ccal regulates several arms of the signaling network in matrix-detached cells as shown in Fig. 5 (numbers in red): (1) Spike in cytosolic calcium (Ccal) activates AMPK via CaMKKβ. (2) Ccal spike activates cAMP which in turn activates PKA. (3) Spike in Ccal activates DAG and IP3; DAG activates PKC which in turn inhibits IRS and subsequent PI3K/Akt signaling pathway. (4) Activated AMPK inhibits the Akt signaling pathway; low levels of pAkt is neither able to activate the mTOR/S6K1 axis, nor auto-activate IRS/PI3K axis. (5) Further, reduced levels of pAkt results in decreased translocation of GLUT1 to the membrane. (6) Additionally,

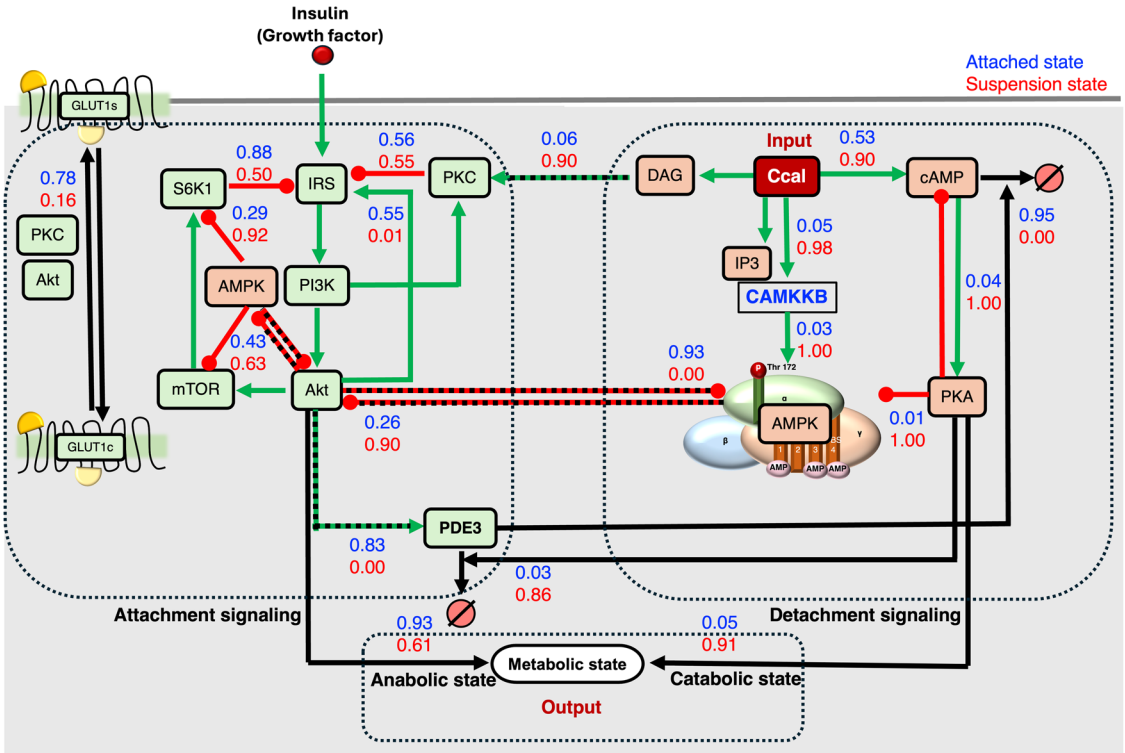

Fig. 5 | Flux map in matrix-attached (blue) and matrix-deprived (red) condition. Numbers along the feedbacks and crosstalks indicate the magnitude of activation or inhibition in terms of the corresponding hill function values, which lie between 0 and 1. The matrix-attached state is marked by high levels of pAkt and low levels of aPKA which contributes to high anabolic state and low catabolic state, respectively and the matrix-deprived state is marked by low levels of pAkt and high levels of aPKA levels which contributes to mild anabolic state and high catabolic state, respectively.

reduced levels of pAkt prevents the inhibition on AMPK and activation of PDE3. Low levels of aPDE3 is unable to degrade cAMP, hence there is a rise in levels of cAMP. High levels of cAMP activates PKA. Though the flux map shows PKA's inhibition on AMPK, still pAMPK levels remain high, perhaps due to strong activation via upstream kinase CaMKKβ triggered by matrix detachment.

Furthermore, the status of the crosstalks in the matrix-deprived state reveals an opposite trend as compared to matrix-attached condition. The crosstalk from catabolic to anabolic pathway (i.e., DAG to PKC) is fully functional, which indicates high levels of PKC and subsequently, high inhibition of IRS. This manifests into low levels of pAkt. Conversely, the crosstalk from anabolic to catabolic pathway (i.e., Akt to PDE3) is switched off, which indicates low levels of aPDE3 and subsequently, accumulation of cAMP. This manifests into high levels of aPKA. Additionally, the crosstalk from Akt to AMPK is non-functional and the crosstalk from AMPK to Akt is fully functional. Therefore, in the matrix-deprived state, the anabolic signaling is reduced wherein pAkt levels are lowered with higher levels of pAMPK, resulting in high aPKA indicating a catabolic state. Also, the lowered anabolic state reduces GLUT1 at the membrane indicating lowered glucose uptake. Thus, the above flux map captures the signaling/metabolic status of matrix-detached cells.

Mathematical network analysis identifies critical feedback and crosstalks for metabolic switching upon matrix deprivation

The previous section depicted the dynamics of signaling molecules and their interactions that gave rise to a coordinated signal transduction in matrix-attached and matrix-deprived breast cancer cells (Fig. 4 and Fig. 5). The flux analyses also unveil the functional strengths of various feedbacks and crosstalks (Fig. 5). One crucial event that occurs during the transition from matrix-attached to matrix-detached condition is the metabolic switching. This is indicated in Fig. 3h by a drop in the anabolic state (blue line) and a rise in catabolic state (red line) upon induction of matrix deprivation (indicated by the black arrow). The cross-over of the blue and red lines indicates metabolic switching from anabolic to catabolic state. We now queried the significance of the various feedbacks and crosstalks that may contribute to this metabolic switching upon matrix-deprivation. To do so, we delinked one feedback or crosstalk at a time (details in Methods section), and noted its effect on the metabolic switching as the system transitions from the matrix-attached to the matrix-deprived state. The solid lines in Fig. 6 represent the unperturbed state as shown in Fig. 3h, while the dotted lines in Fig. 6 show the effect of delinking.

We first queried what happens to the matrix detachment-induced metabolic switch when the positive feedback from DAG to PKC is removed (Fig. 6a). To do so, we delinked DAG to PKC and simulated the model in the matrix-attached state for the first 10 min, and thereafter in the matrix-detached state. We observed that the anabolic state (Fig. 6a; dotted blue line) shows an upward shift as compared to the unperturbed condition (Fig. 6a; solid blue line), while the catabolic state (Fig. 6a; dotted red line) does not exhibit a significant shift as compared to the unperturbed (Fig. 6a; solid red line). These results indicate that the delinking from DAG to PKC results in the retention of anabolic state even upon matrix deprivation, while not affecting the catabolic state. The absence of crossover between the dynamics of the anabolic and catabolic counterparts (dotted blue and red lines) upon DAG to PKC delinking indicates that the metabolic switching is curbed (Fig. 6a). Further, the retention of the anabolic state upon matrix deprivation may be attributed to the enhanced levels of pAkt (Fig. 6b; dotted black line) as compared to its unperturbed counterpart (Fig. 6b; solid black line). The absence of significant change in the dynamics of the catabolic state upon matrix deprivation is attributed to the reduced levels of aPKA (Fig. 6c; dotted black line) as compared to its unperturbed counterpart (Fig. 6c; solid black line). This reduction in aPKA does not affect the catabolic state.

Taken together, these analyses reveal that the crosstalk from DAG to PKC is crucial for the metabolic switching upon matrix-detachment. Similar results are obtained when negative feedback from S6K1 to IRS is removed

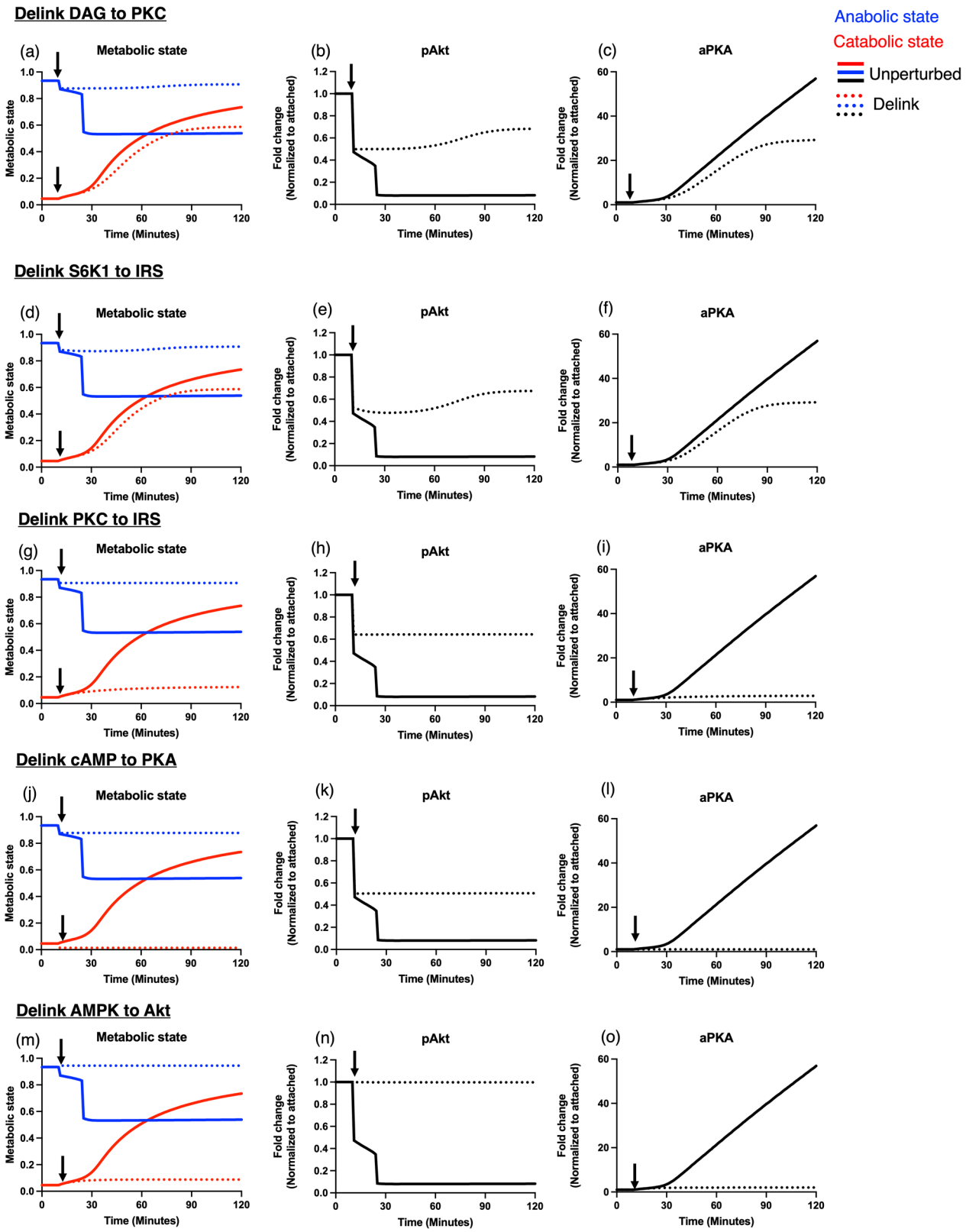

Fig. 6 | Effects of molecular perturbations on the metabolic state (first column) and temporal dynamics of pAkt and aPKA (second and third column). a–c Delink DAG to PKC, **d–f** Delink S6K1 to IRS, (**g–i**) Delink PKC to IRS, (**j–l**) Delink cAMP to PKA and (**m–o**) Delink AMPK to Akt. The graphs are plotted for 120 minutes. The black arrow indicates the time point when matrix deprivation is induced via the spike in cytosolic calcium. The x-axis depicts time in minutes, where, first 10 minutes is the matrix-attached state and remaining is the matrix-deprived state. The y-axis depicts the metabolic state as well as fold change of protein levels, normalized to protein levels in the matrix-attached condition. The solid blue line denotes anabolic state and solid red line denotes catabolic state of unperturbed condition. The dotted blue line denotes anabolic state post-delinking and red dotted line denotes catabolic state post-delinking. The solid black line denotes temporal dynamics of pAkt and aPKA in unperturbed state and dotted black line denotes temporal dynamics of pAkt and aPKA post-delinking.

(Fig. 6d–f). Both (DAG to PKC and S6K1 to IRS) of these delinks ultimately facilitate the increase in levels of pIRS, which enhances the levels of pAkt and hence the high anabolic state, without affecting the catabolic state.

When the negative feedback from PKC to IRS was delinked, we observed that the anabolic state (Fig. 6g; dotted blue line) shows an upward shift as compared to unperturbed (Fig. 6g; solid blue line). However, we observed that upon delinking, the catabolic state (Fig. 6g; dotted red line) exhibits a downward shift as compared to unperturbed (Fig. 6g; solid red line).This indicates that the delinking from PKC to IRS influences the retention of both anabolic state and catabolic state upon matrix deprivation in the similar range as matrix attachment. The absence of crossover between the dynamics of the anabolic and catabolic states upon PKC to IRS delinking indicates that the metabolic switching is curbed (Fig. 6g).The retention of the anabolic state upon matrix deprivation is attributed to the enhanced levels of pAkt (Fig. 6h; dotted black line) as compared to its unperturbed counterpart (Fig. 6h; solid black line). The greater reduction of the catabolic state upon matrix deprivation is attributed to the low levels of aPKA (Fig. 6i; dotted black line) as compared to its unperturbed counterpart (Fig. 6i; solid black line). Therefore, the crosstalk from PKC to IRS is crucial for the metabolic switching.

The delinking from PKC to IRS (Fig. 6g–i) also contributes to increased pIRS which enhances pAkt and facilitates the anabolic state. However, it is interesting to note that aPKA plunges to a very low level, which contributes to the low catabolic state. A difference is noticed in aPKA levels when S6K1 to IRS is delinked (Fig. 6f) as compared to when PKC to IRS is delinked (Fig. 6i). Though pIRS levels remain unchanged (Supplementary Fig. 2a) for these two delinkings, a difference is noticed in the levels of aPDE3 (Supplementary Fig. 2b) and cAMP (Supplementary Fig. 2c). This highlights the auto-inhibitory loop that exists between cAMP and PKA, i.e., cAMP activates PKA, however, PKA inhibits cAMP. Additionally, aPDE3 degrades cAMP which further reduces aPKA. Conversely, aPKA degrades aPDE3. Hence, IRS emerges as an interesting node which impacts the catabolic state upon delinking from PKC and S6K1, but its molecular interplay with cAMP, PDE3 and PKA need further experimental examination.

We next queried what happens when cAMP to PKA is delinked. Similar trend as above is observed upon delinking the positive feedback from cAMP to PKA. Though, the decrease in aPKA (Fig. 6l) is straightforward, but the increased level of pAkt (Fig. 6k) is non-trivial. It is possible that decreased levels of aPKA leads to the accumulation of aPDE3, thus rendering pAkt redundant. This may cause pAkt to be maintained at an increased level upon delinking as compared to unperturbed. This also opens new avenues for exploration along PKA-Akt axis. Both PKA and Akt are powerful indicators of metabolic states as indicated in our study, however, it will be interesting to explore the connection between the two. Literature evidence shows that PKA inactivates CaMKKβ[29]. Though we know that CaMKKβ activates AMPK and AMPK inhibits Akt, the rational for enhanced levels of pAkt and hence high levels of anabolic state upon delinking cAMP to PKA needs further experimental examination.

When the negative feedback from AMPK to Akt is delinked, similar trend in metabolic output is observed as with, delinking of PKC to IRS and cAMP to PKA. However, the distinguishing feature in this case of delinking is the maximum levels of pAkt. This is attributed to the removal of the inhibition by AMPK, which is a strong inhibitory interaction on Akt. The anabolic state is high due to high levels of pAkt (Fig. 6n) and this indirectly contributes to the low levels of aPKA (Fig. 6o) via PDE3 and cAMP, thus conferring the low catabolic state.

Hence, the above five feedback/crosstalks are essential to cause the metabolic switching which serves as an adaptation to survival of matrix-deprived breast cancer cells. The remaining delinking experiments (Supplementary Fig. 3) resemble the dynamics of metabolic state as the unperturbed condition. These feedbacks are as follows: PKA to PDE3, PDE3 to cAMP, PKA to AMPK, Akt to IRS, Akt to PDE3, AMPK to mTOR, AMPK to S6K1 and Akt to AMPK. When these feedbacks/crosstalks are delinked the metabolic switch from catabolic to anabolic is observed similar to unperturbed. When Akt to PDE3 is delinked, the metabolic switching is delayed but attains steady state by 240 min. Hence, these feedbacks/crosstalks may not affect the metabolic switching upon matrix deprivation.

Additionally, since AMPK and Akt reciprocally negate each other, the interaction between AMPK and Akt constitutes a double-negative feedback loop[10]. Towards understanding this through our model, we performed bistability analysis. However, we did not find the system to be distinctly bistable (Supplementary Fig. 4) with respect to the input (Ccal). This may be due the fact that the attachment-detachment signaling is governed by several other feedbacks and crosstalks in addition to the double-negative feedback loop between AMPK and Akt. And the cumulative effect of all crosstalks and feedbacks that forms an integrated network among the signaling molecules diminishes the property of bistability imparted by the double-negative feedback loop.

The model predicts the effects of down-modulation of AMPK on several signaling molecules of the network upon matrix deprivation

Previous work from our laboratory showed that $pAMPK^{High}/pAkt^{Low}$ phenotype, which is a consequence of matrix deprivation, is critical for cell survival in suspension[10], our laboratory also showed that down-modulation of AMPK led to elevated levels of pAkt and exhibited anabolic state in suspension[10]. To study the importance of AMPK on the attachment-detachment signaling at a systems levels, we examined the effects of down-modulation of AMPK on the dynamics of the identified signaling molecules of the network such as pIRS, pPI3K, pPKC, sGLUT1, IP3, DAG, aPKA cAMP, and aPDE3, followed by a system level flux map analysis. To do so, in silico AMPK knockdown (KD) was performed (see Methods). Following AMPK KD, the model was simulated in the matrix-deprived condition and the dynamics of pAMPK (Fig. 7a), pAkt (Fig. 7b), p-mTOR (Fig. 7c), pS6K1 (Fig. 7d), anabolic state (Fig. 7e) and catabolic state (Fig. 7f) were depicted for 1440 min (24 h). These model outcomes concurred with experimental data[10], and hence, these validation results indicated that the model was able to capture the effects of AMPK KD.

Following this model validation, we wanted to understand whether other signaling molecules are perturbed on AMPK KD. The model predicted an increase in pIRS (Fig. 7g), aPI3K (Fig. 7h), sGLUT1 (Fig. 7j), and aPDE3 (Fig. 7o), and a decline in the levels of DAG (Fig. 7l), aPKA (Fig. 7m), and cAMP (Fig. 7n). Interestingly, the model also shows that pPKC (Fig. 7i) and IP3 (Fig. 7k) are not affected by AMPK KD in matrix-deprived state. This indicated that AMPK plays a role in the regulation of IRS, PI3K, GLUT1, DAG, PKA, cAMP, and PDE3 while not affecting IP3 and PKC. These testable predictions (Fig. 7g–o) need to be validated by further experimental study.

To get a system-level understanding on the effects of AMPK KD, the MBCS model was used to quantify the strength of the various interactions of the signaling network as described previously (Fig. 5). The numbers written along the arrows in Fig. 8 indicate the operational strengths of the feedbacks and crosstalks, in the matrix-attached (values in blue) and matrix-detached (values in red) conditions, upon AMPK KD.

When AMPK is down-modulated, the resultant flux map in the matrix-deprived state (Fig. 8, numbers in red), is observed to be different from the flux map in matrix-deprived state when AMPK is unperturbed (Fig. 5; numbers in red values). The matrix deprivation-triggered spike in cytosolic calcium activates CaMKKβ and subsequently CaMKKβ is ready to activate AMPK and stimulate downstream signaling events. However, AMPK down-modulation affects the signaling network of the matrix-deprived state in the following way: (1) AMPK's inhibitory effect on Akt falls drastically. (2) This leads to increased levels of pAkt, which maximally inhibits any remaining AMPK. (3) High levels of pAkt contributes to (a) activation of mTOR/S6K1 axis, (b) auto-phosphorylates and activates IRS, (c) enhances the translocation of GLUT1 to the surface, as well as (d) activates PDE3. (4) High levels of aPDE3 contributes to degradation of cAMP which results in reduced activation of PKA.

Therefore, upon AMPK down-modulation the decreased PKA activity contributes to a reduction in the catabolic state while increased Akt activity

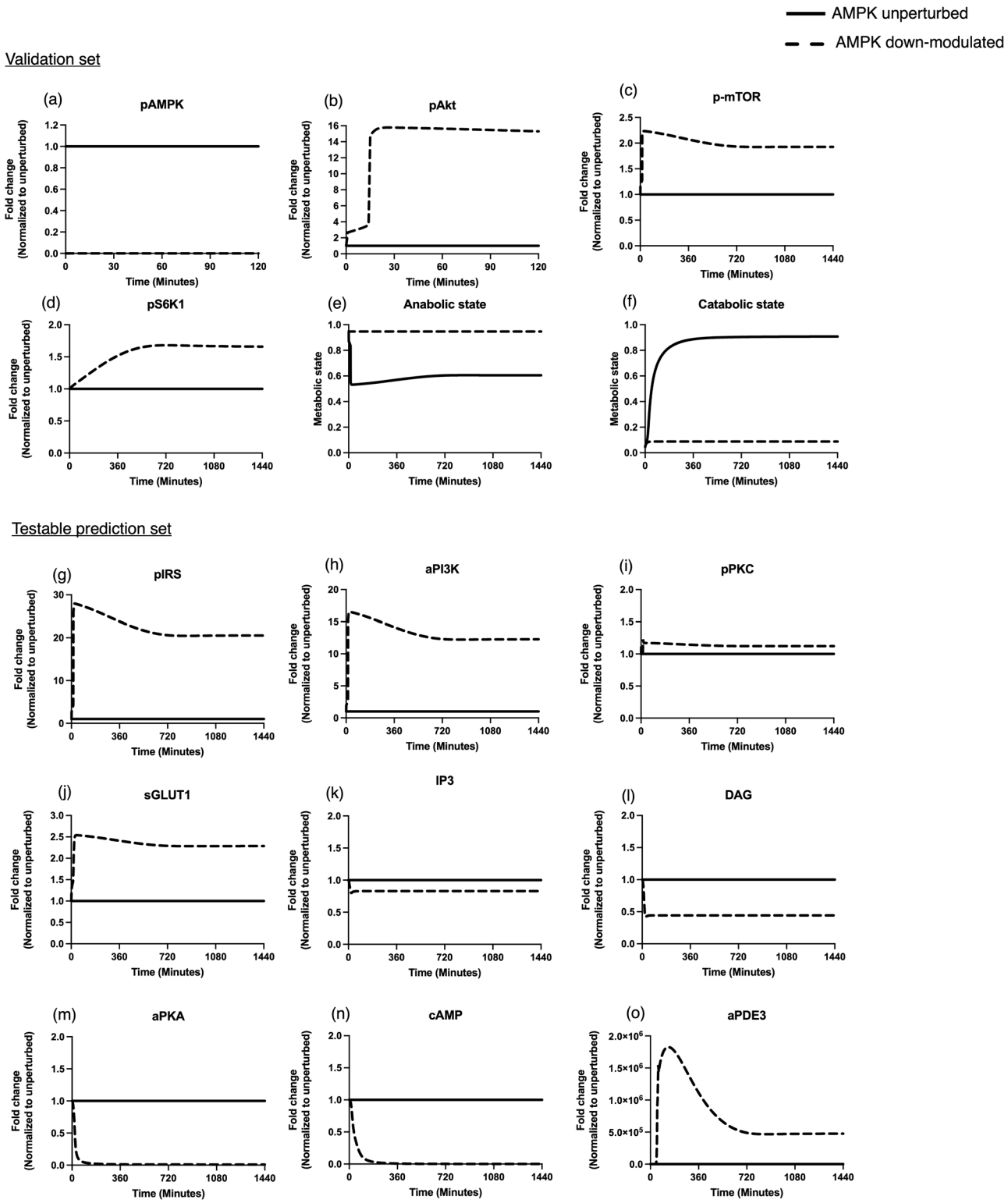

Fig. 7 | Temporal dynamics of molecular players in matrix-deprived condition. Effect of AMPK down-modulation on (**a**) pAMPK, (**b**) pAkt, (**c**) p-mTOR, (**d**) pS6K1 (**e**) Anabolic state, (**f**) Catabolic state, (**g**) pIRS, (**h**) aPI3K, (**i**) pPKC, (**j**) sGLUT1, (**k**) IP3, (**l**) DAG, (**m**) aPKA, (**n**) cAMP and (**o**) aPDE3. The x-axis shows time in minutes. The y-axis depicts fold change of signaling molecules normalized to unperturbed AMPK condition. The solid black line shows the dynamics for unperturbed AMPK, and the dashed black line shows the dynamics for down-modulated AMPK.

contributes to an enhanced anabolic state, hence preventing the metabolic switching. Yet another interesting observation is that, upon down-modulation of AMPK, the flux map in the matrix-deprived state (Fig. 8; numbers in red values) resembles the flux map in the matrix-attached state (Fig. 8; numbers in blue values). This indicates that AMPK KD prevents the change in the signal transduction of matrix-deprived state and retains the signaling consistent with matrix-attached state. This highlights the significance of AMPK in regulating a signaling cascade conducive for cell survival upon matrix detachment which falls apart upon AMPK KD. Furthermore, the flux map upon AMPK KD (Fig. 8) shares a stark similarity

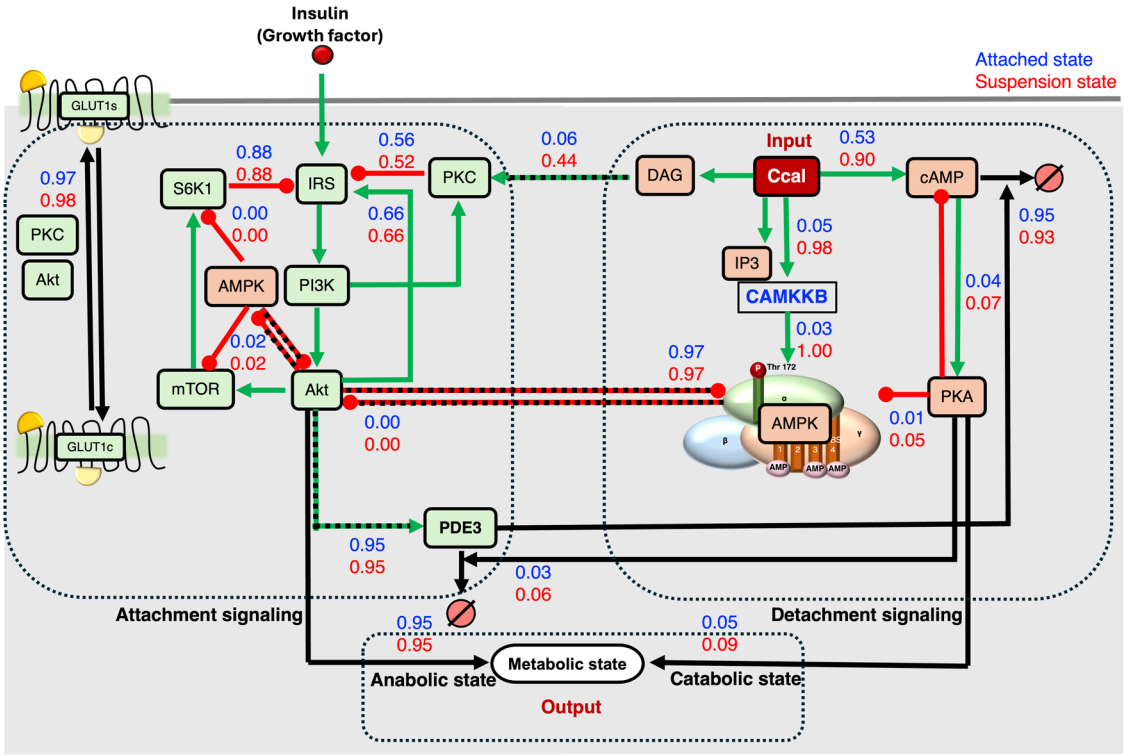

Fig. 8 | Flux map for effect of down-modulation of AMPK in matrix-attached (blue) and suspended (red) condition. Numbers along the feedbacks and crosstalks indicate the magnitude of activation or inhibition in terms of the corresponding hill function values, which lie between 0 and 1. In both matrix-attached and suspended, high levels of pAkt contribute to increased anabolic state and low levels of active PKA contributes to reduced catabolic state.

with the flux map of matrix-attached state when AMPK is unperturbed (Fig. 5; numbers in blue values). The similarity in these flux maps can be rationalized by the fact that AMPK does not play a significant role in matrix-attached state, and this is consistent with its least activity in adherent condition.

Hence, the model outcomes (Figs. 7 and 8) further emphasize that AMPK activation is the key switch upon matrix deprivation, and its down-modulation prevents the metabolic switching and resembles a signal transduction of matrix-attached. These data further suggest that targeting AMPK is likely to prevent cancer cell survival in suspension by preventing the signaling-metabolic rewiring, and hence mitigate metastasis.

Since the model was able to capture the effects of down-modulation of AMPK, which is similar to the matrix-attached state, we were keen to explore whether the model can recapitulate the physiology of re-attachment that occurs at the metastatic site for new tumor growth. Prior experimental data (Supplementary Fig. 5) from our laboratory showed that the levels of pAMPK and pAkt upon re-attachment resembled the trend seen in matrix-attached state. We performed in silico experiment to study the dynamics of metabolic state when matrix deprivation is reversed or re-attachment is induced. This experiment was performed by assigning the steady state values of suspension as initial conditions at 480 min and resetting the fold change of cytosolic calcium to attached condition. Supplementary Fig. 6a shows that metabolic state shifts to the highly anabolic range while Supplementary Fig. 6b shows that metabolic state shifts to the low catabolic range upon induction of re-attachment. Hence, the above experiment revealed that the model is able to capture the effects of re-attachment on the metabolic state of matrix-deprived cancer cells.

Discussion

A critical event in the spread of cancer by metastasis involves detachment from the primary site and survival in the circulation without ECM-attachment by activating anoikis-resistance mechanisms. This attachment-detachment cascade of metastasis is complex and involves co-ordination among several signaling molecules as well as metabolic reprogramming. Towards resolving this complexity, mathematical models serve as promising tools. Albeit there are several mathematical models of breast cancer[15–20], to the best of our knowledge, there exists none that elucidates the attachment-detachment signaling during cancer metastasis. In this study, we utilized the matrix detachment-triggered calcium spike and consequent robust activation of AMPK[9] as the starting point to begin to model signalling events and metabolic outcomes in response to matrix deprivation. This experimentally-driven mathematical model captures the pathophysiology of matrix-deprived state in breast cancer cells by elucidating the perturbation in signaling network and metabolic phenotype that may contribute towards cellular adaptations to survive the stress due to matrix deprivation.

Upon matrix detachment, cells undergo changes in multiple signaling pathways including integrin transduction and its downstream pathways such as: Ras-ERK, PI3K-Akt, YAP-TAZ that contribute towards anchorage-independent survival[7]. It is interesting to note that while cellular detachment and its effects on integrin and growth factor receptors, and consequent effects on Akt has been studied[7,9,10], the effect of detachment on GPCR signaling and PKA activation remains unexplored. Our study revealed various changes in cAMP, DAG, IP3, PKA, which are downstream to GPCR-PKA signaling axis. Though major part of the proposed signaling network follows canonical signaling event as reported previously[10,21], we have identified a few non-canonical pathways based on our model. Our network exhibited the activation of DAG/PKC axis, cAMP/PKA axis, and IP3 by the spike in Ccal. Literature shows the presence of canonical pathway of calcium signaling wherein DAG and IP3 are upstream to calcium signaling which gets activated via GPCR signaling[28]. However, literature also shows the existence of both regulation of cAMP/PKA signaling by calcium and regulation of calcium signaling by cAMP/PKA pathway in a rather interesting system of secretory epithelium[30]. Increase in intracellular concentration of calcium has also been shown to trigger the association of PKC with the membrane where DAG interacts with PKC to stimulate the enzyme activity[31]. There are also speculations that increased cytosolic calcium levels

may induce positive feedback that activates PLC to cleave PIP2 into IP3 and DAG[32]. Though the above interactions have not been reported in the context of breast cancer, the possibility of such interactions strengthens our proposed model. Another interesting observation that emerges from the flux map analysis is the observed maximum strength of AMPK activation by CaMKKβ in the matrix-deprived state despite the presence of aPKA that has inhibitory effects on AMPK[33,34](Fig. 5). However, what masks the effect of aPKA on AMPK is not clearly understood. Perhaps in the matrix-deprived state, the inhibition of AMPK by aPKA is not functional, or the activation of AMPK by CAMKKβ is dominant; these need further experimental explorations.

While matrix deprivation has been known to affect the activity of AMPK, Akt, mTOR, S6K1, PKC and PKA, our study unveiled several additional testable predictions which may serve as hypotheses for experimental/modeling studies to enhance our understanding of metastatic breast cancer. For example, the MBCS model predicted the effects of matrix deprivation on pIRS, aPI3K, sGLUT1, DAG, IP3, cAMP and aPDE3. Literature shows evidence for a few of these predictions, but concrete data is unavailable. For example, glucose uptake is known to be reduced in the matrix-deprived cancer cells[35]. Loss of attachment of non-transformed mammary epithelial cells (MCF-10A) from ECM caused a deficiency in ATP due to reduced glucose uptake. This phenotype was rescued by introduction of constitutively active variant of PI3K or Akt[36]. This indirectly indicates that aPI3K may deplete in suspension state. Along the same lines, our model also predicts the decrease in aPI3K levels upon matrix deprivation. PI3K/Akt signaling regulates both the expression of glucose transporter GLUT1 mRNA and the translocation of GLUT1 protein to the plasma membrane, thus acting as a master regulator of glucose uptake[37]. Albeit this correlation, the status of GLUT1 on the cell membrane of breast cancer cells in the matrix-deprived state remains unclear. Our model predicts a decrease in sGLUT1 in the matrix-deprived state; however, this needs to be investigated rigorously. PKC is a serine-threonine kinase which is known as pleotropic regulator of cell proliferation, differentiation and survival[38]. Experimental data from our laboratory showed that there were no detectable differences in the levels of pPKC between matrix-deprived state as compared to attached condition (Supplementary Fig. 1). Supporting the same, our model also predicted that pPKC levels remain unaltered. PKA, commonly known as cAMP-dependent protein kinase, is an enzyme essential for several intracellular signal transduction and maintenance of cellular homeostasis. PKA is known to tightly regulate metabolism via G-protein coupled receptors (GPCRs)[39]. Interestingly, PKA activation promoted cancer cell resistance to glucose starvation and anoikis[27]. PKA activation was stronger in suspension cells when compared to adherent cells[27]. Along the same lines, our model also predicts an increase in PKA activity. Furthermore, the model also predicts a decrease in the levels of pIRS, aPDE3, and an increase in the levels of IP3, DAG and cAMP. However, the status of these proteins and secondary messengers in matrix-deprived condition has not been elucidated yet.

AMPK is known to aid in stress survival of matrix-deprived cancer cells[8,10,40]. The MBCS model revealed that down-modulation of AMPK is associated with increase in levels of pIRS, aPI3K, sGLUT1, pAkt, p-mTOR and pS6K1 which may be counterproductive under the stress of matrix deprivation. Additionally, the model also revealed reduction in levels of aPKA upon AMPK knockdown. PKA is known to exert protective role to suspension cells[27]. Thus, in silico down-modulation of AMPK reveals several factors that are detrimental to the survival of matrix-deprived breast cancer cells.

Accumulating evidence supports the existence of dynamic metabolic rewiring in metastasizing cancer cells[41]. Anabolic outcomes are expected to be heightened in the attached state where Akt is active, and catabolic outcomes are expected to be heightened in the matrix-deprived state where PKA is active[10,27]. Though our results exhibit the above phenomena, it is interesting to note that the MBCS model predicts the presence of mild anabolic state in the matrix-detached condition in addition to high catabolic state. In support of this, some literature also supports the existence of simultaneous glycolysis (anabolic) and gluconeogenesis (catabolic) activities in hepatocytes[42]. It is not clearly understood whether anabolic state coexist with catabolic state in the matrix-deprived breast cancer cells, warranting more studies in this direction. Interestingly, recent work from our laboratory showed that though matrix deprivation and AMPK activation inhibits global protein translation, yet protein synthesis (an anabolic process) continues in matrix-detached cells[22]. Since mTOR is inactivated in suspension, we speculate that matrix-detached cells utilize alternate (non-cap-dependent) modes of protein translation, and indeed our recent study shows evidence for the presence of an altered translatome that might aid cancer cell survival in matrix-deprived condition[22]. Additionally, molecular perturbations also revealed the significance of several feedbacks and crosstalks to maintain desired metabolic state via activation Akt and PKA. Thus, the MBCS model begins to give insights into possible metabolic re-wiring to aid metastasis.

While the model recapitulated the experimental observations based on our prior data[9,10], we do acknowledge certain limitations of the study. Firstly, for a more comprehensive understanding of the complex biological and mechanical events that entail the loss of matrix detachment, this model needs to be further elaborated to include components of integrin-FAK and growth factor signalling, cell mechanics involving YAP-TAZ signalling, and force development among others. Secondly, for a better understanding of the metabolic phenotypes, the model needs to include inputs of altered metabolism and components of bioenergetics. In the present work, we have only looked at the signaling pathway where the phosphorylation status of Akt and activation of PKA are correlated to metabolic phenotype of the cell. In future, this could be modified to incorporate metabolic networks including glycolysis, oxidative phosphorylation, amino acid and fatty acid metabolism, and TCA cycle, along with the signaling network. Thirdly, the experimental data available on matrix deprivation are not conducive for temporal modeling due to fewer time points. This poses challenge to utilize standard optimization algorithms for parameter estimation. Future work will require generation of data at multiple time points to enable accurate model fitting by automated methods.

Despite the above limitations, the developed MBCS model widely captures the attachment-detachment signaling of breast cancer cells. This model can be further benchmarked to other subtype-specific breast cancers by including the dominant signaling pathways of each subtype. It can be extrapolated to study the phenomenon of matrix deprivation in other solid cancers as well. Moreover, this model can be further used to incorporate different cell fates like apoptosis by including Akt's interaction with cytochrome C and caspase 3. Each of these may serve as starting point to hypothesize subsequent experimental/modeling studies and aid in a systematic approach to understand and curb the metastatic cancer spread.

Methods

Experimental data extraction

In vitro experimental data retrieved from previously published work of our laboratory was used for model calibration and validation. The calibration set consisted of the data on effects of matrix deprivation on spike in cytosolic calcium[9], and levels of pAMPK[10], pAkt[10] and p-mTOR[22]. The validation set consisted of the data on effects of matrix deprivation on levels of pS6K1, pPKC, and aPKA, effects on metabolic state (anabolic vs catabolic) and down-modulation of AMPK in MDA-MB-231 cells[10,22]. The representative images of the published western blot data were re-quantified using ImageJ software.

Mathematical Methods

The current model integrated previously validated[21] adipocyte-based mechanistic model on insulin-glucagon signaling network with experimental data on matrix-detached breast cancer cells to generate a mathematical model to study breast cancer metastasis. The ordinary differential equations (ODEs) were formulated based on kinetic rate laws and mass balance of signaling proteins. Hill functions were used to capture important feedback and crosstalks in the network (details in Supplementary

Information). Dynamic solutions of these ODEs were obtained using ODE15s solver in MATLAB. The steady-state profiles of the proteins were obtained and compared across matrix-attached and matrix-deprived conditions.

Determination of system metrics

Defining individual metabolic state. The output of the model was described in the form of metabolic state. The metabolic state was independently quantified by anabolic state and catabolic state of the cells which was attributed to the phosphorylation status of Akt and activation of PKA. Hence, the anabolic state was defined as:

$$\text{Anabolic state} = \frac{\text{pAkt}}{h_{\text{pAkt}} + \text{pAkt}}$$

And the catabolic state was defined as:

$$\text{Catabolic state} = \frac{\text{aPKA}}{h_{\text{aPKA}} + \text{aPKA}}$$

Where, h_{aPKA} and h_{pAkt} were the half saturation thresholds for the signaling components. The extent of catabolic (aPKA) and anabolic (pAkt) states were characterized by the above equations.

Calculating flux maps. To visualize the relative operational strengths of the feedback and crosstalks under matrix-attached and matrix-deprived conditions, the absolute values of the corresponding Hill functions were evaluated and plotted in the flux maps as reported in the Results section.

Delinking experiments

Delinking was performed by setting each of the Hill functions to either 0.05 or 0.95, based on whether the Hill function is located in the phosphorylation arm or the dephosphorylation arm. For example, to delink DAG to PKC, we considered that DAG activates PKC and upon delinking, PKC should no longer be activated by DAG. Mathematically, PKC should not rise post-delinking. Since the effect of DAG on PKC was included in the phosphorylation arm of PKC, the corresponding Hill function was set to 0.05 to enable delinking. Delinking of other feedbacks/crosstalks were performed using the same rationale.

In silico AMPK knockdown

In silico AMPK knockdown or down-modulation of AMPK was performed by maintaining pAMPK at a very low level. Briefly, down-modulation of AMPK was performed by setting the ordinary differential equation of pAMPK to zero. This ensured that the rate of change of pAMPK remains zero. Subsequently, the initial value of pAMPK was set at 0.0001, which ensured the levels of pAMPK remains very low. This was done to disable the dynamics of pAMPK or induce down-modulation of AMPK in silico.

Data availability

All the data generated or analyzed during this study are included in this article and its Supplementary Information.

Received: 1 February 2024; Accepted: 23 September 2024;
Published online: 12 November 2024

References

1. Hanahan, D. Hallmarks of Cancer: New Dimensions. *Cancer Discov.* **12**, 31–46 (2022).
2. Sung, H. et al. Global Cancer Statistics 2020: GLOBOCAN Estimates of Incidence and Mortality Worldwide for 36 Cancers in 185 Countries. *CA. Cancer J. Clin.* **71**, 209–249 (2021).
3. Chaffer, C. L. & Weinberg, R. A. A Perspective on Cancer Cell Metastasis. *Science* **331**, 1559–1564 (2011).
4. Winkler, J., Abisoye-Ogunniyan, A., Metcalf, K. J. & Werb, Z. Concepts of extracellular matrix remodelling in tumour progression and metastasis. *Nat. Commun.* **11**, 5120 (2020).
5. Yu, J. S. L. & Cui, W. Proliferation, survival and metabolism: the role of PI3K/AKT/mTOR signalling in pluripotency and cell fate determination. *Development* **143**, 3050–3060 (2016).
6. Frisch, S. & Francis, H. Disruption of epithelial cell-matrix interactions induces apoptosis. *J. Cell Biol.* **124**, 619–626 (1994).
7. Deng, Z., Wang, H., Liu, J., Deng, Y. & Zhang, N. Comprehensive understanding of anchorage-independent survival and its implication in cancer metastasis. *Cell Death Dis.* **12**, 629 (2021).
8. Hindupur, S. K. et al. Identification of a novel AMPK-PEA15 axis in the anoikis-resistant growth of mammary cells. *Breast Cancer Res.* **16**, 420 (2014).
9. Sundararaman, A., Amirtham, U. & Rangarajan, A. Calcium-Oxidant Signaling Network Regulates AMP-activated Protein Kinase (AMPK) Activation upon Matrix Deprivation. *J. Biol. Chem.* **291**, 14410–14429 (2016).
10. Saha, M. et al. AMPK–Akt Double-Negative Feedback Loop in Breast Cancer Cells Regulates Their Adaptation to Matrix Deprivation. *Cancer Res.* **78**, 1497–1510 (2018).
11. Hardie, D. G. Keeping the home fires burning: AMP-activated protein kinase. *J. R. Soc. Interface* **15**, 20170774 (2018).
12. Hardie, D. G., Schaffer, B. E. & Brunet, A. AMPK: An Energy-Sensing Pathway with Multiple Inputs and Outputs. *Trends Cell Biol.* **26**, 190–201 (2016).
13. Anderson, A. R. A., Chaplain, M. A. J., Newman, E. L., Steele, R. J. C. & Thompson, A. M. Mathematical Modelling of Tumour Invasion and Metastasis. *J. Theor. Med.* **2**, 129–154 (2000).
14. Franssen, L. C., Lorenzi, T., Burgess, A. E. F. & Chaplain, M. A. J. A Mathematical Framework for Modelling the Metastatic Spread of Cancer. *Bull. Math. Biol.* **81**, 1965–2010 (2019).
15. Mohammad Mirzaei, N. et al. A Mathematical Model of Breast Tumor Progression Based on Immune Infiltration. *J. Pers. Med.* **11**, 1031 (2021).
16. He, W., Demas, D. M., Conde, I. P., Shajahan-Haq, A. N. & Baumann, W. T. Mathematical modelling of breast cancer cells in response to endocrine therapy and Cdk4/6 inhibition. *J. R. Soc. Interface* **17**, 20200339 (2020).
17. Jarrett, A. M. et al. Experimentally-driven mathematical modeling to improve combination targeted and cytotoxic therapy for HER2+ breast cancer. *Sci. Rep.* **9**, 12830 (2019).
18. Damaghi, M. et al. The harsh microenvironment in early breast cancer selects for a Warburg phenotype. *Proc. Natl. Acad. Sci. USA* **118**, e2011342118 (2021).
19. Jia, D. et al. Elucidating cancer metabolic plasticity by coupling gene regulation with metabolic pathways. *Proc. Natl. Acad. Sci. USA* **116**, 3909–3918 (2019).
20. Chedere, A., Hari, K., Kumar, S., Rangarajan, A. & Jolly, M. K. Multi-Stability and Consequent Phenotypic Plasticity in AMPK-Akt Double Negative Feedback Loop in Cancer Cells. *J. Clin. Med.* **10**, 472 (2021).
21. Somvanshi, P. R., Tomar, M. & Kareenhalli, V. Computational Analysis of Insulin-Glucagon Signalling Network: Implications of Bistability to Metabolic Homeostasis and Disease states. *Sci. Rep.* **9**, 15298 (2019).
22. Warrier, S., Srinivasan, S., Chedere, A. & Rangarajan, A. Inhibition of protein translation under matrix-deprivation stress in breast cancer cells. *Front. Med.* **10**, 1124514 (2023).
23. Petersen, M. C. & Shulman, G. I. Mechanisms of Insulin Action and Insulin Resistance. *Physiol. Rev.* **98**, 2133–2223 (2018).
24. Aronoff, S. L., Berkowitz, K., Shreiner, B. & Want, L. Glucose Metabolism and Regulation: Beyond Insulin and Glucagon. *Diabetes Spectr.* **17**, 183–190 (2004).
25. Jiang, G. & Zhang, B. B. Glucagon and regulation of glucose metabolism. *Am. J. Physiol. -Endocrinol. Metab.* **284**, E671–E678 (2003).

26. Tegge, A. N., Sharp, N. & Murali, T. M. X TALK: a path-based approach for identifying crosstalk between signaling pathways. *Bioinformatics* **32**, 242–251 (2016).
27. Palorini, R. et al. Protein Kinase A Activation Promotes Cancer Cell Resistance to Glucose Starvation and Anoikis. *PLOS Genet* **12**, e1005931 (2016).
28. Clapham, D. E. Calcium Signaling. *Cell* **131**, 1047–1058 (2007).
29. Zhang, H., Kong, Q., Wang, J., Jiang, Y. & Hua, H. Complex roles of cAMP–PKA–CREB signaling in cancer. *Exp. Hematol. Oncol.* **9**, 32 (2020).
30. Ahuja, M., Jha, A., Maléth, J., Park, S. & Muallem, S. cAMP and Ca2+ signaling in secretory epithelia: Crosstalk and synergism. *Cell Calcium* **55**, 385–393 (2014).
31. Huang, K.-P. The mechanism of protein kinase C activation. *Trends Neurosci.* **12**, 425–432 (1989).
32. Bagley, K. C., Abdelwahab, S. F., Tuskan, R. G. & Lewis, G. K. Calcium Signaling through Phospholipase C Activates Dendritic Cells To Mature and Is Necessary for the Activation and Maturation of Dendritic Cells Induced by Diverse Agonists. *Clin. Vaccin. Immunol.* **11**, 77–82 (2004).
33. Djouder, N. et al. PKA phosphorylates and inactivates AMPKα to promote efficient lipolysis. *EMBO J.* **29**, 469–481 (2010).
34. Ferretti, A. C. et al. AMPK and PKA interaction in the regulation of survival of liver cancer cells subjected to glucose starvation. *Oncotarget* **7**, 17815–17828 (2016).
35. Grassian, A. R., Coloff, J. L. & Brugge, J. S. Extracellular Matrix Regulation of Metabolism and Implications for Tumorigenesis. *Cold Spring Harb. Symp. Quant. Biol.* **76**, 313–324 (2011).
36. Schafer, Z. T. et al. Antioxidant and oncogene rescue of metabolic defects caused by loss of matrix attachment. *Nature* **461**, 109–113 (2009).
37. Pavlova, N. N. & Thompson, C. B. The Emerging Hallmarks of Cancer Metabolism. *Cell Metab.* **23**, 27–47 (2016).
38. Garg, R. et al. Protein kinase C and cancer: what we know and what we do not. *Oncogene* **33**, 5225–5237 (2014).
39. London, E., Bloyd, M. & Stratakis, C. A. PKA functions in metabolism and resistance to obesity: lessons from mouse and human studies. *J. Endocrinol.* **246**, R51–R64 (2020).
40. Jeon, S.-M., Chandel, N. S. & Hay, N. AMPK regulates NADPH homeostasis to promote tumour cell survival during energy stress. *Nature* **485**, 661–665 (2012).
41. Bergers, G. & Fendt, S.-M. The metabolism of cancer cells during metastasis. *Nat. Rev. Cancer* **21**, 162–180 (2021).
42. Phillips, J. W., Jones, M. E. & Berry, M. N. Implications of the simultaneous occurrence of hepatic glycolysis from glucose and gluconeogenesis from glycerol. *Eur. J. Biochem.* **269**, 792–797 (2002).

Acknowledgements

We acknowledge Manipa Saha and Ananthalakshmy Sundararaman for critical discussion on experimental data that was used to build this mathematical model. We also thank Abha Saxena and Manoj Srivatsn for helping with MATLAB code. SM acknowledges the Prime Minister Research Fellowship (PMRF). Funds from Wellcome Trust DBT India Alliance Senior Research Fellowship (500112-Z-09-Z to AR) and funds from the DBT-IISc partnership programme of the Department of Biotechnology, Govt of India, for experimental data used in this manuscript are acknowledged. Infrastructural support from the UGC to the Department of DBG is also acknowledged.

Author contributions

S.M., A.R., and K.V. conceived and designed the study. S.M. constructed the model in MATLAB, performed the computer simulations, assembled and analyzed the data, and drafted the manuscript. S.M., A.R., and K.V. were involved in interpreting results and critical discussion. A.R. and K.V. edited and revised the manuscript.

Competing interests

The authors declare no completing interests.

Additional information

Supplementary information The online version contains supplementary material available at https://doi.org/10.1038/s41540-024-00443-4.

Correspondence and requests for materials should be addressed to Annapoorni Rangarajan or Venkatesh Kareenhalli.